Chemogenetic protein engineering: an efficient tool for the optimization of artificial metalloenzymes

Anca Pordea and Thomas R. Ward*†

Received (in Cambridge, UK) 21st April 2008, Accepted 11th June 2008
First published as an Advance Article on the web 12th August 2008
DOI: 10.1039/b806652c

Artificial metalloenzymes, based on the incorporation of a catalytically active organometallic moiety within a host protein, lie at the interface between organometallic and enzymatic catalysis. In terms of activity, reaction repertoire, substrate range and operating conditions, they take advantage of the versatility of the organometallic chemistry. In contrast, the enantioselectivity is determined by the biomolecular scaffold, which provides a well defined second coordination sphere to the organometallic moiety, reminiscent of enzymes. The attractive feature of such systems is their optimization potential, which combines chemical and genetic methods (*i.e.* chemogenetic) to screen diversity space. This feature article describes the implementation of such an optimization protocol for artificial transfer hydrogenases, for which we have the most detailed understanding.

Introduction

In the area of high value-added chemicals, enantioselective catalysis plays an ever-increasing role.[1,2] Catalysis has traditionally been divided into three distinct fields: heterogeneous, homogeneous and enzymatic catalysis. The latter two have found most applications in enantioselective catalysis.[3,4] Despite intensive computational, structural and mechanistic studies, predicting the outcome of an enantioselective catalytic transformation remains very challenging. This is due to the fact that a difference in free energy of only 2.0 kcal mol^{-1} for the two diastereomeric transition states affords an enantiomeric excess (ee) of 95%.[5] Thus, subtle, weak non-bonding contacts between the substrate and the catalytic environment often play a decisive role in the enantioselection. This has led to the implementation of combinatorial strategies in homogeneous catalysis' optimization.[6–9] For this purpose, a library of ligands is combined with a suitable metal precursor and screened in the presence of various additives, counter ions, co-solvents *etc.*[10]

In contrast to homogeneous catalysts, enzymes offer an exquisitely tailored and well-defined second coordination sphere, which often leads to outstanding selectivities for an enzyme's native substrate.[11] Broadening an enzyme's substrate scope or inverting its enantioselectivity often requires a major

Institute of Chemistry, University of Neuchâtel, Avenue Bellevaux 51, CP158, CH-2009 Neuchâtel, Switzerland. E-mail: thomas.ward@unine.ch; Fax: +41 32 718 2511; Tel: +41 32 718 2516
† *Present address*: Department of Chemistry, University of Basel, Spitalgasse 51, CH-4056 Basel, Switzerland. E-mail: thomas.ward@unibas.ch; Fax: +41 61 267 1005; Tel: +41 61 267 1004.

Anca Pordea

Anca Pordea, born in Arad (Romania), obtained her diploma in Organic Chemistry from the National Institute of Applied Sciences (INSA) of Rouen (FR). She carried out her PhD research in Prof. Thomas R. Ward's group at the University of Neuchâtel (CH), where she focused on the creation and optimization of artificial metalloenzymes. She is currently a Swiss National Science Foundation post-doctoral fellow in the group of Prof. Benjamin G. Davis at the University of Oxford (UK).

Thomas R. Ward

Thomas R. Ward, born in Fribourg (Switzerland), received his diploma in Chemistry from the University of Fribourg and his PhD from the ETH Zurich. After post-doctoral work at Cornell University and at the University of Lausanne, he moved to Berne as an independent researcher, obtaining his Venia Legendi. From 2000 to 2008, he worked at the University of Neuchâtel and moved to the University of Basel in March 2008. The group's research is centered on the exploitation of proteins as hosts for organometallic moieties with applications in catalysis as well as in nanobiotechnology.

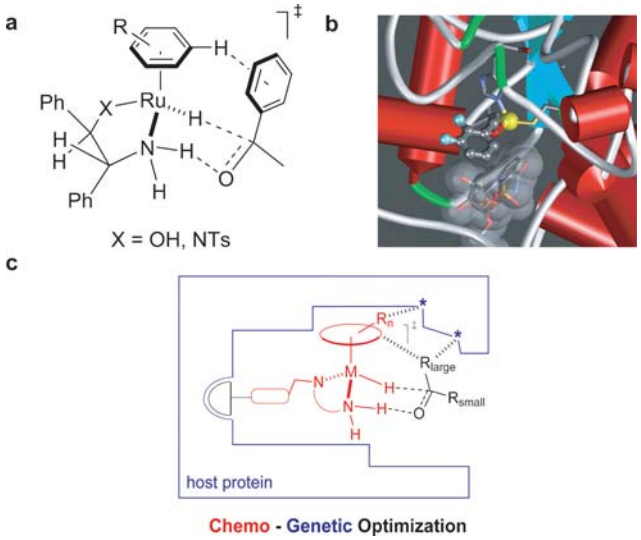

Fig. 1 (a) Computed transition state structure for the transfer hydrogenation of aromatic ketones using Ru d^6 piano-stool complexes (adapted from ref. 33). The $C_{aromatic}H$–π attraction between the η^6-arene and the aromatic substituent is at the origin of enantioselectivity. (b) Structure of the active site of an alcohol dehydrogenase containing a substrate molecule. The oxygen atom of the substrate is directly coordinated to the zinc atom, while the side chain interacts with the hydrophobic cavity of the protein, PDB refcode 1QV7. (c) Artificial metalloenzymes for the transfer hydrogenation of prochiral ketones based on supramolecular anchoring. The host protein displays high affinity for the anchor; chemical optimization is performed by introduction of a spacer and variation of the d^6 piano-stool moiety; site-directed mutagenesis of the host protein allows the genetic optimization.

optimization effort. This is best achieved by directed evolution strategies, which however require screening of large libraries.[12–14] In many ways (optimization, substrate scope, solvent tolerance, reaction repertoire *etc.*), enzymes and homogeneous catalysts are often considered as complementary.

In addition to metal-mediated (*e.g.* homogeneous) and enzymatic catalysis, organocatalysis (minimal enzymes)[15] and artificial metalloenzymes[16–19] have attracted renewed interest in recent years.

The creation and optimization of artificial metalloenzymes, which are the focus of this feature article, aim at combining the most appealing features of homogeneous and enzymatic catalysis. Their design is based on the chemical modification of a protein with a catalytically active organometallic moiety. Such systems offer the possibility of optimizing both the first and the second coordination sphere around the catalytically active metal (Fig. 1). The first coordination sphere, provided by the organometallic moiety itself by-and-large determines the activity of the catalyst and may readily be optimized by chemical means, using methods reminiscent of homogeneous catalyst optimization. The second coordination sphere, provided by the host protein may, in turn, be optimized with genetic means.[16,20–23] Ideally, one could envision creating an artificial metalloenzyme for nearly any water-compatible transition metal-catalyzed reaction,[24] thus broadening the scope of enzymatic catalysis.

Inspired by Whitesides' early report,[25] we focused on artificial metalloenzymes based on the biotin–(strept)avidin technology. Here, (strept)avidin refers to either avidin or streptavidin, where (strept)avidin is a tetrameric protein possessing four identical binding pockets, which have a very high affinity for biotin. A well-tailored hydrogen-bonding net, as well as precise hydrophobic interactions with aromatic residues are responsible for the biotin-(strept)avidin binding, which ranks among the strongest non-covalent interactions known ($K_d \sim 10^{-15}$ M).[26] Most importantly, modification of the valeric acid side chain of biotin does not lead to a significant decrease in the affinity constant.[26] In the context of organometallic catalysis, we speculated that non-covalent anchoring of a biotinylated organometallic fragment into the host protein should ensure the integrity of the organometallic species and may occur with a tolerable erosion in the affinity constant.[27]

The potential of these hybrid catalysts was initially tested for the hydrogenation of α-acetamidoacrylic acid using rhodium–diphosphine complexes, which proceeded with high enantioselectivities (96% ee (*R*)).[28] Following this initial breakthrough, we extended this methodology to transfer hydrogenation,[29] allylic alkylation[30] as well as alcohol[31] and sulfide[32] oxidation reactions. In this feature article, we outline our efforts towards the creation of artificial transfer hydrogenases for which we have the most detailed understanding.

Artificial transfer hydrogenases: a case study

Enantiopure alcohols are important intermediates in the synthesis of various high value-added chemicals.[34] The asymmetric reduction of prochiral ketones is perhaps the most straightforward route to access this class of compounds. Both enzymatic[35,36] and homogeneous catalysis[34,37,38] have been widely used to achieve this transformation.

The asymmetric transfer hydrogenation based on d^6 piano-stool complexes is an attractive alternative to reduction systems using molecular hydrogen.[39–43] Mechanistic studies suggest that both the hydride and the proton transfer proceed through a concerted six-membered transition state, without coordination of the prochiral substrate to the metal (Fig. 1(a)).[44,45] In nature, oxidoreductases such as liver alcohol dehydrogenase catalyze the reduction of carbonyl compounds with remarkable enantioselectivities using organic cofactors such as NAD(P)H.[4] In these enzymatic systems, enantiodiscrimination is controlled by the second coordination sphere interactions between the substrate and the enzyme (Fig. 1(b)).

With the aim of creating new hybrid systems for enantioselective reduction, we chose the Noyori-type asymmetric transfer hydrogenation of ketones as a model reaction, which relies on d^6 piano-stool complexes as catalysts. Considering the nature of the critical non-covalent interactions within the transition state (Fig. 1(a) and (c)), we reasoned that the second coordination sphere contacts between the host protein and the substrate may lead to good selectivities, even for challenging substrates. Most importantly, recent examples in the field of chemo-enzymatic catalysis demonstrated the compatibility between d^6 piano-stool metal complexes and enzymatic systems at elevated temperatures, thus suggesting that biotinylated piano-stool complexes may perform their task in the presence of streptavidin acting as a host protein.[46]

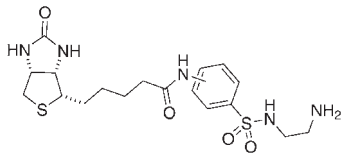

Scheme 1 General structure of the *ortho*-, *meta*- and *para*-biotinylated ligands (**Biot-*q*-L**H) used in this study.

The catalytic system

The first step in the implementation of the new artificial transfer hydrogenation system was the identification of the suitable reaction conditions for the enantioselective reduction of acetophenone used as a model substrate.[29]

In conjunction with d^6 piano-stool complexes, Noyori and co-workers have shown that aminosulfonamides are among the most effective ligands for the enantioselective transfer hydrogenation of aromatic ketones.[38,41] Thanks to their water compatibility and stability,[47] they represent attractive candidates for our purposes. Derivatization of an aromatic aminosulfonamide with a biotin anchor can readily be achieved *via* an amide functionality to afford the biotinylated ligands **Biot-*q*-L**H (*q* = *ortho*-, *meta*- or *para*-, Scheme 1). These ligands were mixed with $[\eta^6$-(*p*-cymene)$RuCl_2]_2$ in the presence of a base to afford the catalyst precursor [η^6-(*p*-cymene)Ru(**Biot-*q*-L**)Cl]. In the absence of streptavidin, these complexes catalyzed the aqueous transfer hydrogenation of acetophenone to yield (*rac*)-phenylethanol in quantitative yield. Addition of streptavidin to the catalytic system introduces a delicate component against which the influence of every reagent present was evaluated. For this purpose, we used [η^6-(*p*-cymene)Ru(**Biot-*p*-L**)Cl]⊂WT Sav as a model artificial transfer hydrogenase. Throughout the paper, WT Sav refers to wild-type streptavidin and the inclusion symbol ⊂ indicates the non-covalent incorporation of the biotinylated catalyst within streptavidin. All the results presented herein were obtained using homo-tetrameric Sav and mutants thereof.

Hydrogen source. Isopropanol (*i*PrOH), formic acid–triethylamine azeotropic mixture or aqueous sodium formate (HCOONa) are the most common hydrogen sources for transfer hydrogenation. Non-denaturing gel electrophoresis of the reaction mixture carried out in the presence of these hydrogen donors revealed the presence of monomeric streptavidin, suggesting that they denature the protein. Since it had been shown that the reduction rates are considerably faster using HCOONa than the HCOOH–Et_3N azeotrope or *i*PrOH,[48] the former was selected for further optimization. Decreasing the formate concentration from 1.5 to 0.5 M suppressed the denaturation of the host protein, ensuring that the chiral environment remained unaltered throughout catalysis.

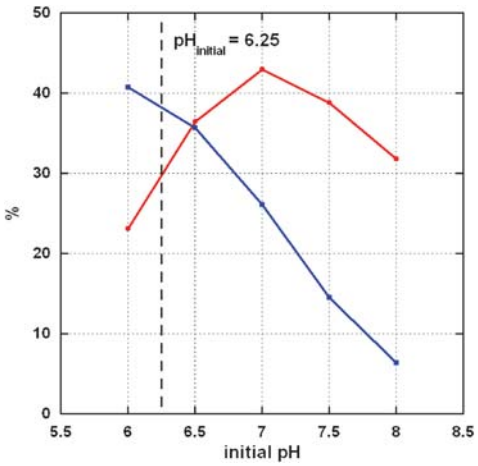

Fig. 2 Variation of the conversion (red circles) and of the ee (blue squares) as a function of the initial pH for the reduction of acetophenone using [η^6-(*p*-cymene)Ru(**Biot-*p*-L**)Cl]⊂WT Sav. *Reaction conditions*: WT Sav (tetrameric) 45 μM; Ru 130 μM; HCOONa 1.5 M; acetophenone 0.013 M; temperature 45 °C; reaction time 45 h.

pH. Studies by the groups of Ogo and Xiao had shown that both the reaction rate and the enantioselectivity of aqueous transfer hydrogenation reactions critically depend on the pH of the reaction.[49,50] A study of the activity and selectivity of the reaction as a function of the initial pH allowed us to identify pH = 6.25 as the optimum for catalysis in the presence of artificial transfer hydrogenases (Fig. 2).[22] Given the pK_a^1 = 3.75 of formic acid and bearing in mind that the pH of an ampholyte at its isoelectric point is given by pH = 0.5 (pK_a^1 + pK_a^2), we screened various acids with a $pK_a^2 \approx 8.75$. This allowed to identify HCOONa·$B(OH)_3$ as the best combination both in terms of activity and of selectivity (Table 1, entry 1). The addition of MOPS buffer contributed to further stabilize the pH throughout catalysis ($pH_{initial}$ = 6.25; $pH_{final} < 7.3$), thus increasing the selectivity at the expense of a slightly lower conversion (Table 1, entry 2).

Temperature. With the aim of increasing the conversion, the temperature and the reaction time were increased. Using the mixed HCOONa·$B(OH)_3$ + MOPS buffer at 55 °C, the

Table 1 Optimization of the reaction conditions for the asymmetric transfer hydrogenation of acetophenone **1** catalyzed by [η^6-(*p*-cymene)-Ru(**Biot-*q*-L**)Cl]⊂WT Sav[a]

Entry	Ligand	Buffer system ($pH_{initial}$ = 6.25)	*T*/°C	*t*/h	Conv. (%)	ee (%)
1	**Biot-*p*-L**	HCOONa·$B(OH)_3$	45	40	55	57 (*R*)
2	**Biot-*p*-L**	HCOONa·$B(OH)_3$ + MOPS[b]	45	40	40	66 (*R*)
3	**Biot-*p*-L**	HCOONa·$B(OH)_3$ + MOPS[b]	55	64	82	68 (*R*)
4	**Biot-*p*-L**	HCOONa·$B(OH)_3$ + MOPS[b]	65	64	76	66 (*R*)
5	**Biot-*m*-L**	HCOONa·$B(OH)_3$	45	40	20	6 (*S*)
6	**Biot-*o*-L**	HCOONa·$B(OH)_3$	45	40	18	3 (*S*)

[a] *Conditions*: WT Sav (tetrameric) 45 μM; Ru 130 μM; HCOONa 0.5 M; $B(OH)_3$ 0.47 M; acetophenone **1** 0.013 M. [b] WT Sav (tetrameric) 36 μM; Ru 104 μM; HCOONa 0.48 M; $B(OH)_3$ 0.41 M; MOPS 0.16 M; acetophenone **1** 0.01 M.

Table 2 Selected results for the chemogenetic optimization of the performance of [η^6-(arene)Ru(**Biot-*p*-L**)Cl]⊂Sav for the transfer hydrogenation of acetophenone derivatives **1–3**[a]

Entry	η^6-Arene	Protein	Substrate	Conv. (%)	ee (%)
1	*p*-Cymene	WT Sav	**1**	82	68 (*R*)
2[b]	*p*-Cymene	WT Sav	**2**	93	87 (*R*)
3[b]	*p*-Cymene	WT Sav	**3**	86	91 (*R*)
4[b]	Benzene	WT Sav	**1**	54	48 (*S*)
5	*p*-Cymene	P64G Sav	**1**	90	85 (*R*)
6	*p*-Cymene	P64G Sav	**3**	92	94 (*R*)
7[c]	*p*-Cymene	S112G Sav	**1**	90	28 (*R*)

[a] *Conditions*: WT Sav (tetrameric) 36 μM; Ru 104 μM; HCOONa 0.48 M; $B(OH)_3$ 0.41 M; MOPS 0.16 M; substrate 0.01 M; $pH_{initial}$ = 6.25; temperature 55 °C; reaction time 64 h. [b] WT Sav (tetrameric) 36 μM; Ru 120 μM; substrate 0.012 M. [c] HCOONa 0.5 M; $B(OH)_3$ 0.47 M; temperature 45 °C; reaction time 40 h.

conversion was raised to 82% within 64 h, with little influence on the enantioselectivity (Table 1, entry 3). Further increasing the temperature to 65 °C did not improve the outcome of the reaction (Table 1, entry 4).

Organic co-solvent. The typical reaction was carried out in a buffer solution containing less than 1.5% DMF (v/v), required to dissolve the ruthenium complex and the substrate. Other water-miscible solvents such as DMSO or *i*PrOH worked equally well. Increasing the percentage of organic solvent above 5% had a negative effect on the conversion however.

Using the conditions identified above, the reduction of acetophenone **1** in presence of [η^6-(*p*-cymene)Ru(**Biot-*p*-L**)Cl]⊂WT Sav proceeded with moderate conversion (82%) and enantioselectivity (68% (*R*), Table 1, entry 3). *para*-Bromoacetophenone **2** and *para*-methylacetophenone **3** afforded higher conversions and selectivities (see Scheme 3 and Table 2, entries 2–3).

Ligand structure. The position of the biotinylated catalyst within streptavidin, which was determined by the substitution pattern of **Biot-*q*-L** had a dramatic effect on the outcome of the reaction. The *para*-anchored ligand outperformed the *meta*- and *ortho*-substituted counterparts both in terms of conversion and of selectivity (Table 1, entries 1, 5 and 6). It is tempting to speculate that the *meta*- and *ortho*-anchoring localize the ruthenium centre in a position that is not easily accessible for the substrate.

Nature of the capping arene. In addition to the position of the biotin-anchor with respect to the aromatic aminosulfonamide moiety, the nature of the capping arene was found to play a crucial role in determining both the activity and the selectivity of [η^6-(arene)Ru(**Biot-*p*-L**)Cl]⊂WT Sav. Most unexpectedly, substitution of the η^6-(*p*-cymene) by a η^6-(benzene) cap produced the opposite enantiomer of phenylethanol, under otherwise identical reaction conditions. (Table 2, entries 1 and 4). This initial finding suggests an important interaction between the protein and the ruthenium complex.

To rationalize this observation, two complementary enantioselection mechanisms can be envisaged. First, the absolute configuration at ruthenium in the hydride piano stool complex may be controlled by second coordination sphere interactions with streptavidin. This differs from classical Noyori-type catalysts where the Ru-configuration is determined by the chirality of the chelating ligand scaffold.[51] Second, additional contacts between the substrate and the protein may compete (matched or mismatched) with interactions between the substrate and the η^6-capping arene to favour the approach of one enantiotopic face of the substrate. These two possible enantiodiscriminating events are outlined in Scheme 2 for the (*R*)-selective
[η^6-(*p*-cymene)Ru(**Biot-*p*-L**)Cl]⊂WT Sav combination. For simplification, only the monomer containing the biotinylated Ru complex was represented, although interactions of the adjacent monomer with the Ru complex or the substrate may also be involved.

Protein variants. The optimization potential by introduction of point mutations within the host protein was evaluated next. For this purpose, a glycine residue was introduced in several

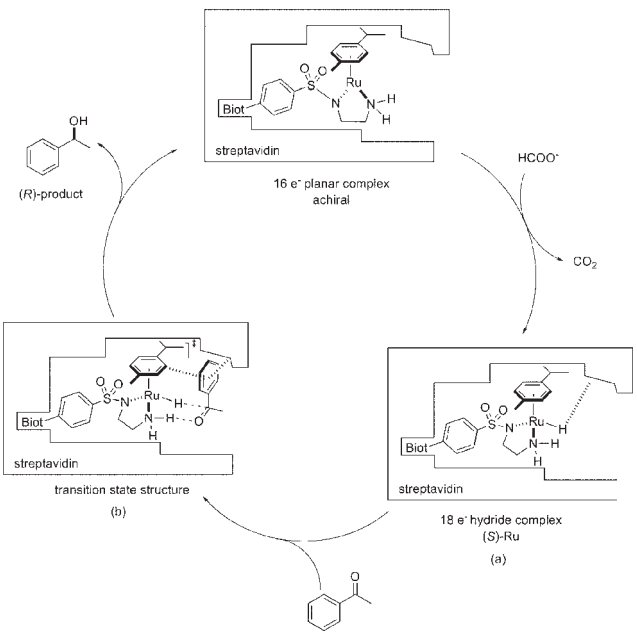

Scheme 2 Suggested weak contacts critical for the observed enantioselectivity in the reduction of acetophenone catalyzed by [η^6-(*p*-cymene)Ru(**Biot-*p*-L**)H]⊂WT Sav. (a) The absolute configuration at Ru may be determined by second coordination sphere contacts between the biotinylated catalyst and streptavidin. (b) The preferential delivery of one enantiotopic face of the substrate may be biased by second coordination sphere interactions between the substrate and streptavidin.

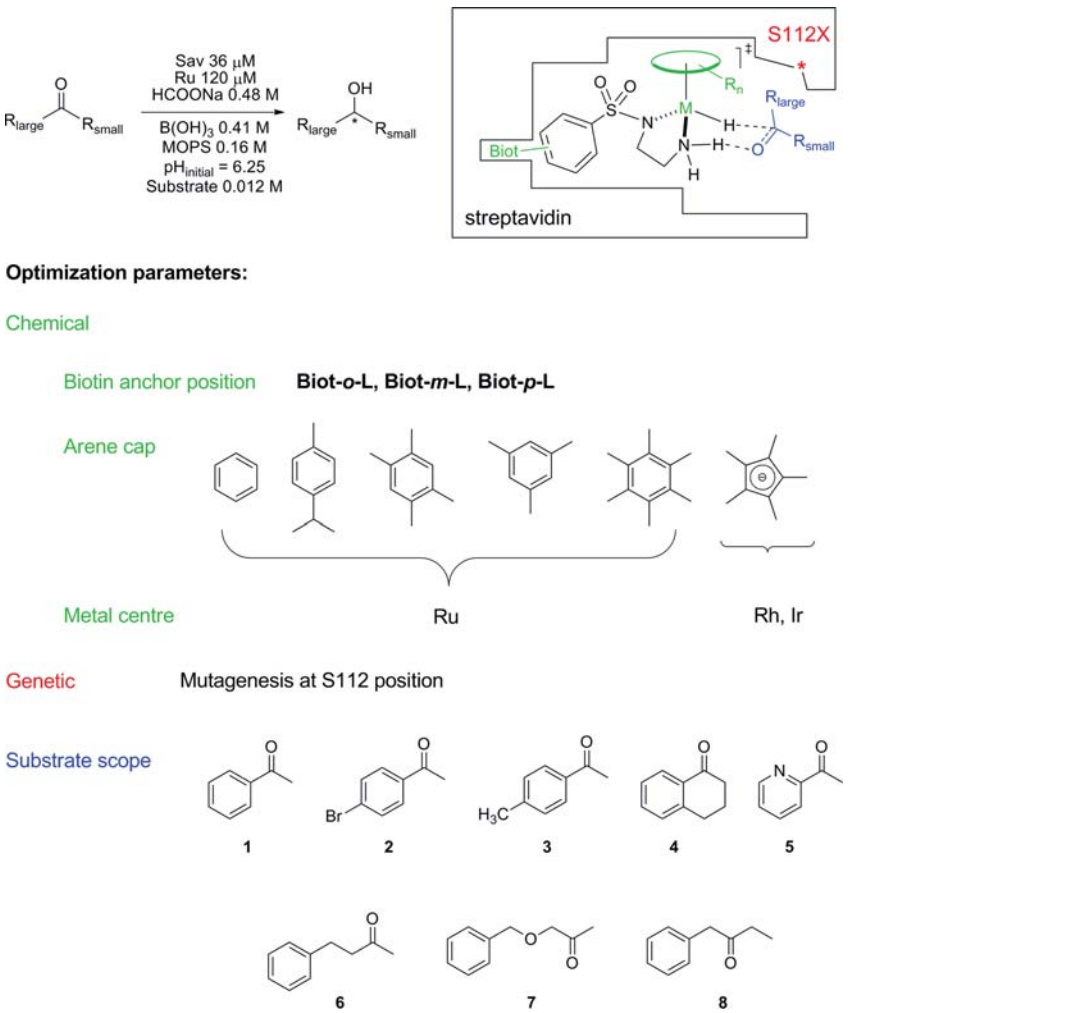

Scheme 3 Chemical, genetic and substrate diversity used for the chemogenetic optimization of enantioselective artificial transfer hydrogenases.

positions to yield single-point mutants (K80G Sav, S112G Sav, V47G Sav and P64G Sav). Interestingly, the protein with the most remote site of mutation (P64G Sav) significantly increased enantioselectivity, while the closest lying mutation (S112G Sav) afforded the greatest variation in enantioselectivity as well as the highest conversions (Table 2, entries 5–7).

This first screening round suggested that both chemical and genetic methodologies could be implemented for the optimization of the artificial transfer hydrogenases.

First round of evolution: exploring the active site

With the aim of broadening the substrate scope and gaining mechanistic insight into the new system, a library of chemically and genetically modified catalyst variants was produced and screened for activity and selectivity for the reduction of prochiral ketones. As no high-throughput methodology was implemented, we focused on minimal modifications at the active site, likely to dramatically affect the reaction outcome: the position of the biotin-anchor, the capping arene and the metal, as well as the residues predicted to lie close to the active site.[22]

Screening strategy. In order to limit the number of screening experiments, we opted for a representational search strategy (positional scanning)[6] to optimize the activity and selectivity of the artificial metalloenzymes. Three variables are expected to have an important effect on the reaction outcome: chemical diversity (catalyst structure), genetic diversity (protein environment) and substrate (Scheme 3). Successive optimization rounds were carried out by modifying a single parameter at a time. The influence of the biotinylated catalyst structure on the asymmetric transfer hydrogenation for the three acetophenone derivatives **1–3** was evaluated first. Then, changes of the host protein through targeted mutations were explored by screening with the most promising organometallic scaffolds. Finally, the scope of the reaction was assessed using the best catalyst⊂protein combinations. While this approach does not take into account the possible cooperativity effects between the different factors (metal complex, protein and substrate), it allows the identification of selective catalysts using a modest screening effort.

Chemical optimization. The biotinylated metal complex was modified by varying the capping arene, the position of the biotin anchor and the metal centre. A total of twenty-one catalyst precursors was generated by combining the three different ligands (*ortho*-, *meta*- and *para*-biotinylated sulfonamides **Biot-*q*-L**H) with seven d^6 piano-stool fragments containing five arene caps and three different metals

(η^5-(C_5Me_5)RhCl, η^5-(C_5Me_5)IrCl and η^6-(arene)RuCl, arene = *p*-cymene, benzene, durene, mesitylene, hexamethylbenzene, Scheme 3). Screening of these catalysts in the presence of streptavidin allowed rapid identification of the most promising metal complexes for the reduction of acetophenone derivatives **1–3**. Two different streptavidin isoforms (WT Sav and P64G Sav) were used in these experiments and the complexes displayed similar trends in both cases. These results suggest that the chemical optimization brings more diversity than the genetic counterpart.[21] The screening experiment further confirmed the initial trends outlined above:

(i) The localization of the catalytic centre, dictated by the position of the biotin anchor, determines the activity of the resulting artificial metalloenzyme: only the *para*-anchored ligands afforded significant levels of conversion.

(ii) The nature of the capping arene plays a critical role in the enantioselectivity: (η^6-(*p*-cymene)-bearing Ru-complexes are mostly (*R*)-selective and η^6-(benzene)-containing Ru-complexes are mostly (*S*)-selective).

Based on these observations, five out of the twenty one biotinylated complexes were selected for further optimization by genetic means: [η^6-(*p*-cymene)Ru(**Biot-*p*-L**)Cl], [η^6-(benzene)-Ru(**Biot-*p*-L**)Cl], [η^6-(durene)Ru(**Biot-*p*-L**)Cl], [η^6-(C_5Me_5)-Ir(**Biot-*p*-L**)Cl] and [η^6-(C_5Me_5)Rh(**Biot-*p*-L**)Cl].

Genetic optimization. To minimize the number of experiments required for an efficient optimization, we focused on modifications close to the active site, assuming that these bring more diversity than the distant ones.[52,53] In the absence of crystallographic information on the exact localization of the catalytic centre, docking studies were performed to obtain a qualitative model of the hybrid catalyst. The most stable docked structure of the ruthenium hydride catalyst [η^6-(*p*-cymene)Ru(**Biot-*p*-L**)H]⊂WT Sav reveals that the two C_α atoms of serine S112 and S122 are the closest lying to the ruthenium moiety. However, the S112 side chain points towards the piano-stool fragment while the S122 side chain is directed away from the complex. These observations and previous results obtained with the S112G Sav mutant, showing the most pronounced changes in conversion and selectivity (Table 2, entry 7), led us to select position S112 for the genetic optimization through saturation mutagenesis. The five biotinylated ruthenium complexes were screened in conjunction with the twenty streptavidin isoforms, S112X Sav. General trends emerged from this second optimization step:

(i) The nature of the capping arene by-and-large determines the preferred enantiomer: (*R*)-reduction products for η^6-(*p*-cymene)- and η^6-(durene)-bearing complexes and (*S*)-reduction products for the η^6-(benzene)-bearing complex (Table 3, entries 1–3 and Fig. 3(a)). The overall performance of the rhodium- and iridium-containing metalloenzymes is modest and depends very much on the host protein (Fig. 3(a)).

(ii) Sav-mutants bearing a potentially coordinating amino acid side chain at position S112 (cysteine, methionine, aspartic or glutamic acid, histidine) inhibit the catalytic performance of the artificial transfer hydrogenases (Table 3, entry 4).

(iii) Introduction of cationic residues at position S112 favours (*S*)-reduction products.

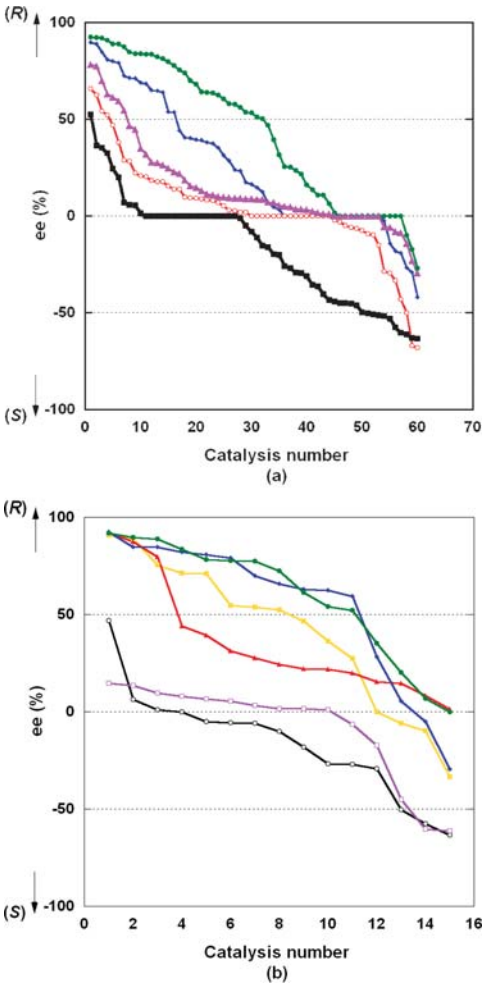

Fig. 3 Summary of the enantioselectivity trends for the first round of chemogenetic optimization, arranged according to: (a) the nature of the complex: [η^6-(*p*-cymene)Ru(**Biot-*p*-L**)Cl] (●), [η^6-(benzene)-Ru(**Biot-*p*-L**)Cl] (■), [η^6-(durene)Ru(**Biot-*p*-L**)Cl] (◆), [η^6-(C_5Me_5)Ir-(**Biot-*p*-L**)Cl] (▲) and [η^6-(C_5Me_5)Rh(**Biot-*p*-L**)Cl] (○); (b) the Sav isoform: S112Y (●), S112F (◆), S112A (■), S112V (▲), S112R (□) and S112K (○).

(iv) Introduction of hydrophobic residues at position S112 favours (*R*)-reduction products.

The latter two trends can act either in a matched or mismatched fashion with either [η^6-(*p*-cymene)Ru(**Biot-*p*-L**)Cl] or [η^6-(benzene)Ru(**Biot-*p*-L**)Cl] to afford good levels of selectivity for (*R*)-reduction products or moderate (*S*)-selectivities (Table 3, entries 5–9 and Fig. 3(b)).

The three acetophenone derivatives display similar trends (up to 92% (*R*) and 62% (*S*), Table 3, entries 2 and 9).

Substrate scope. Having identified the most efficient hybrid catalysts, we proceeded to test substrates **4–8** which are known to be challenging in terms of selectivity for classical transfer hydrogenation reactions (Scheme 3).[54] Dialkyl ketones are challenging as the postulated critical enantiodiscriminating $C_{aromatic}H$–π interaction between the η^6-arene ligand and the substrate's aryl group is absent for substrates **6–8**.[33,55] The five substrates were tested in the presence of the (*R*)-selective catalyst [η^6-(*p*-cymene)Ru(**Biot-*p*-L**)Cl] and the

Table 3 Selected results for the chemogenetic optimization of the transfer hydrogenation of ketones **1–8**[a]

Entry	Protein	Complex	Substrate	Conv. (%)	ee (%)
1	S112Y Sav	[η^6-(*p*-cymene)Ru(**Biot-*p*-L**)Cl]	**1**	95	90 (*R*)
2	S112Y Sav	[η^6-(durene)Ru(**Biot-*p*-L**)Cl]	**2**	88	92 (*R*)
3	S112T Sav	[η^6-(benzene)Ru(**Biot-*p*-L**)Cl]	**2**	90	55 (*S*)
4	S112D Sav	[η^6-(*p*-cymene)Ru(**Biot-*p*-L**)Cl]	**1**	0	—
5	S112A Sav	[η^6-(*p*-cymene)Ru(**Biot-*p*-L**)Cl]	**3**	98	91 (*R*)
6	S112A Sav	[η^6-(benzene)Ru(**Biot-*p*-L**)Cl]	**3**	74	41 (*R*)
7	S112K Sav	[η^6-(*p*-cymene)Ru(**Biot-*p*-L**)Cl]	**1**	50	20 (*S*)
8	S112K Sav	[η^6-(benzene)Ru(**Biot-*p*-L**)Cl]	**1**	37	55 (*S*)
9	S112R Sav	[η^6-(benzene)Ru(**Biot-*p*-L**)Cl]	**3**	23	62 (*S*)
10	S112A Sav	[η^6-(*p*-cymene)Ru(**Biot-*p*-L**)Cl]	**6**	98	48 (*R*)
11	S112A Sav	[η^6-(*p*-cymene)Ru(**Biot-*p*-L**)Cl]	**7**	71	30 (*R*)
12	S112A Sav	[η^6-(*p*-cymene)Ru(**Biot-*p*-L**)Cl]	**8**	97	69 (*R*)
13	S112F Sav	[η^6-(*p*-cymene)Ru(**Biot-*p*-L**)Cl]	**4**	70	96 (*R*)
14	S112K Sav	[η^6-(benzene)Ru(**Biot-*p*-L**)Cl]	**5**	97	70 (*S*)

[a] *Conditions*: WT Sav (tetrameric) 36 μM; Ru 120 μM; HCOONa 0.48 M; $B(OH)_3$ 0.41 M; MOPS 0.16 M; substrate 0.012 M; $pH_{initial}$ = 6.25; temperature 55 °C; reaction time 64 h.

(*S*)-selective catalyst [η^6-(benzene)Ru(**Biot-*p*-L**)Cl]. These were combined with ten representative S112X Sav isoforms (X = A, G and L: aliphatic residues with increasing bulk; F and W: aromatic residues with increasing bulk; S and T: polar residues; E: coordinating anionic residue; R: cationic residue; N: neutral amidic residue) and the best results are summarized in Table 3. The selectivity and conversion trends are similar to those obtained for the acetophenone derivatives **1–3**. Only modest activities and enantioselectivities are obtained with the non-aromatic ketones (Table 3, entries 10–12), suggesting that the 112 position has little influence on determining the orientation of the approaching dialkyl substrates **6–8**. Good selectivities are obtained for α-tetralone (Table 3, entry 13). Interestingly, 2-acetylpyridine **5** afforded the best (*S*)-selectivity in the presence of a cationic residue at the 112 position (up to 70% ee (*S*), Table 3, entry 14). It appears that the presence of a positive charge at this position is particularly beneficial for this substrate. We speculate that the presence of a hydrogen bond between the cationic residue and the pyridine moiety plays a key role in this context.

These results suggest that the chemical modification of the organometallic fragment combined with saturation mutagenesis of a residue close to the computed position of the ruthenium is a powerful tool for the optimization of the artificial transfer hydrogenases. Using this strategy, high (*R*)- and moderate (*S*)-enantioselectivities are obtained for the reduction of several aromatic ketones.

Second round of evolution: X-ray guided designed evolution

Considering the widely accepted enantioselection mechanism (see Fig. 1(a)) between the substrate and the η^6-bound arene, dialkyl ketones are very challenging substrates.[33,55] To circumvent this limitation, Woggon and co-workers tethered a ruthenium piano-stool complex to a β-cyclodextrin, thus providing a pre-organized cavity for the enantioselective transfer hydrogenation of dialkyl substrates (ee up to 95%).[56] Some alternative systems for the asymmetric reduction of selected dialkyl ketones have been developed.[57–62] Undoubtedly however and thanks to directed evolution strategies, alcohol dehydrogenases represent one of the most versatile alternatives to the asymmetric reductions using dihydrogen for the synthesis of optically active aliphatic alcohols.[36] The second coordination sphere of such NAD(P)H-dependent alcohol dehydrogenases is exquisitely tailored to perform regio- and enantioselective reactions of this type.[63]

With the aim of further evolving artificial metalloenzymes by combining structural insight with random mutagenesis to perfect those elements which cannot be predicted—a methodology which we coin designed evolution[64]—we invested a significant effort into crystallizing the most promising artificial transfer hydrogenases. The crystal structure of the (*S*)-selective [η^6-(benzene)Ru(**Biot-*p*-L**)Cl]⊂S112K Sav was determined and provides a fascinating insight on the organization of the active site and of close contacts between the Ru complex and amino acid residues in several loop regions.[65] Interestingly, despite the use of a racemic ruthenium piano-stool complex for crystallization, only the (*S*)-enantiomer of [η^6-(benzene)Ru(**Biot-*p*-L**)Cl] was localized in the crystal structure. In homogeneous systems, the (*S*)-Ru configuration is predicted to afford (*S*)-reduction products. The [η^6-(benzene)-Ru(**Biot-*p*-L**)Cl]⊂S112K Sav was the most (*S*)-selective hybrid catalyst identified during the first screening round (see Fig. 3(b)). This observation supports our hypothesis that second coordination sphere interactions enforce a preferential configuration at ruthenium (Fig. 4). In addition, the short contact between the Ru moieties incorporated into two adjacent monomers suggests that substituting the capping η^6-benzene by a bulkier η^6-*p*-cymene may force the latter biotinylated complex to adopt a different position and/or configuration at the metal to avoid steric hindrance.

This structure confirms the docking results suggesting that S112 position lies in the immediate vicinity of the ruthenium atom. A close contact between the capping arene and the K112 residue of monomer B can also be identified and suggests that the 112_B amino acid might have an influence on the spatial arrangement of the Ru complex inside the host protein. Moreover, in the case of 2-acetylpyridine, the presence of a cationic residue at the 112_B position might lead to hydrogen-bonding contacts between the protein and the substrate, thus privileging the preferred transition state favoured by the $C_{aromatic}H$–π interaction (Fig. 4).

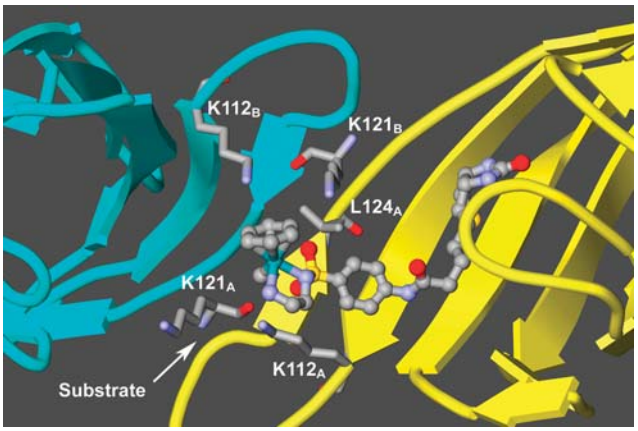

Fig. 4 Close up view of the structure of [η^6-(benzene)Ru(**Biot-*p*-L**)Cl]⊂S112K Sav determined by X-ray crystallography (only one dimer of the tetramer depicted for clarity). Only monomer A was occupied by the biotinylated Ru complex. Residues K112, K121 and L124 of monomer A (yellow) and K112, K121 of monomer B (blue) are highlighted. A possible trajectory of the incoming prochiral substrate is also indicated by an arrow. It should be noted that the occupancy of the metal moiety is only 20%.[65]

A comparison between the computed Ru–C_α distances for the docking model ([η^6-(*p*-cymene)Ru(**Biot-*p*-L**)H]⊂WT Sav) and for the X-Ray structure ([η^6-(benzene)Ru(**Biot-*p*-L**)Cl]⊂S112K Sav) shows that, although different Ru complexes and Sav isoforms were used, the metal moiety displays the same close contacts with the host protein in the two cases (Fig. 5). Two additional close lying amino acid residues are identified: K121 and L124. The first one is of particular interest, as the K121 residues of both monomers A and B can interact either with the η^6-arene (monomer B) or with the expected trajectory of incoming substrate (monomer A). The side chain of the L124 amino acid may influence the position of the biotinylated complex inside the hydrophobic pocket as it lies close to the sulfonamide moiety of **Biot-*p*-L** (Fig. 4).

Guided by the X-ray structure presented above, we implemented a designed evolution protocol to optimize the selectivity for dialkyl ketone substrates as well as to improve the (*S*)-selectivity for acetophenone derivatives. Starting from the previously identified (*R*)- and (*S*)-selective variants, an additional mutation was introduced in the vicinity of the active site. Given the difficulty to predict the effect of a particular amino acid residue on the reaction outcome, once more saturation mutagenesis was performed. The procedure was applied to two different amino acid residues, which we speculate could alter the position of the metal complex within the binding pocket or could steer the delivery of the substrate, thus influencing the enantioselectivity of the reaction.[65]

The two positions selected for the second round of saturation mutagenesis are K121 and L124. They are combined with either the S112A Sav, S112K Sav ((*R*)-, respectively (*S*)-selective mutants), or WT Sav as background. A total of 114 new Sav mutants (K121X; L124X; S112A-K121X; S112A-L124X; S112K-K121X and S112K-L124X) were produced and tested in combination with [η^6-(*p*-cymene)Ru(**Biot-*p*-L**)Cl] and [η^6-(benzene)Ru(**Biot-*p*-L**)Cl] complexes. Dialkyl ketone **6** was chosen as a model substrate, as well as the aromatic substrate **2**.

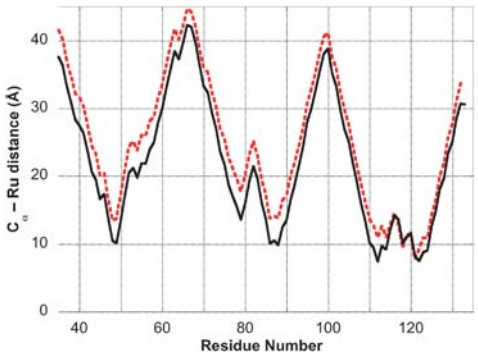

Fig. 5 Comparison between the computed Ru–C_α average distances for [η^6-(*p*-cymene)Ru(**Biot-*p*-L**)H]⊂WT Sav resulting from 135 docking simulations with rms <1 Å (black solid line) and the Ru-C_α distances extracted from the X-Ray structure of [η^6-(benzene)Ru(**Biot-*p*-L**)Cl]⊂S112K Sav (red dotted line); only monomer A containing the Ru complex is represented.

Although the attempts to use Sav-containing cellular extracts in catalysis were unsuccessful, rapid screening of the Sav mutants was achieved using a straightforward extraction–immobilization protocol with biotin-sepharose. Owing to the high affinity of biotin for streptavidin, one biotin-binding site was used for immobilization, leaving up to three free sites to accommodate the biotinylated catalyst.

Using this immobilization strategy, semi-quantitative trends were rapidly obtained for the reduction of 4-phenyl-2-butanone **6** as well as for *p*-bromoacetophenone **2**. The best results using the immobilized hybrid catalysts were subsequently reproduced using a purified Sav mutant in a homogeneous phase. These catalysts were evaluated with substrates **1–8**. From these experiments, the following tendencies emerge:

(i) The enantioselectivity of the reaction is mainly dictated by the chemical moiety (η^6-*p*-cymene *vs.* η^6-benzene), with notable exceptions in the case of the metalloenzymes bearing the S112A mutation ([η^6-(benzene)Ru(**Biot-*p*-L**)Cl]⊂S112A–K121W 84% ee (*R*), Table 4, entry 1).

(ii) Overall, the systems incorporating the S112K mutation are least selective, suggesting that the lysine side chain at

Table 4 Selected results obtained for the designed evolution of artificial transfer hydrogenases for substrates **1–8** using purified and homogeneous artificial oxido-reductases[a]

Entry	Sav mutant	Metal moiety	Substrate	Conv. (%)	ee (%)
1	S112A-K121W	[η^6-(benzene)Ru]	**6**	99	84 (*R*)
2	S112A-K121T	[η^6-(*p*-cymene)Ru]	**6**	99	88 (*R*)
3	S112A-K121T	[η^6-(*p*-cymene)Ru]	**7**	100	90 (*R*)
4	S112A-K121T	[η^6-(*p*-cymene)Ru]	**8**	50	46 (*R*)
5	S112A-K121N	[η^6-(benzene)Ru]	**6**	100	72 (*S*)
6	S112A-K121N	[η^6-(benzene)Ru]	**2**	98	75 (*S*)
7	S112A-K121N	[η^6-(benzene)Ru]	**4**	54	92 (*S*)
8	S112A-K121N	[η^6-(benzene)Ru]	**5**	100	92 (*S*)

[a] *Conditions*: WT Sav (tetrameric) 36 μM; Ru 120 μM; HCOONa 0.48 M; $B(OH)_3$ 0.41 M; MOPS 0.16 M; substrate 0.012 M; $pH_{initial}$ = 6.25; temperature 55 °C; reaction time 64 h.

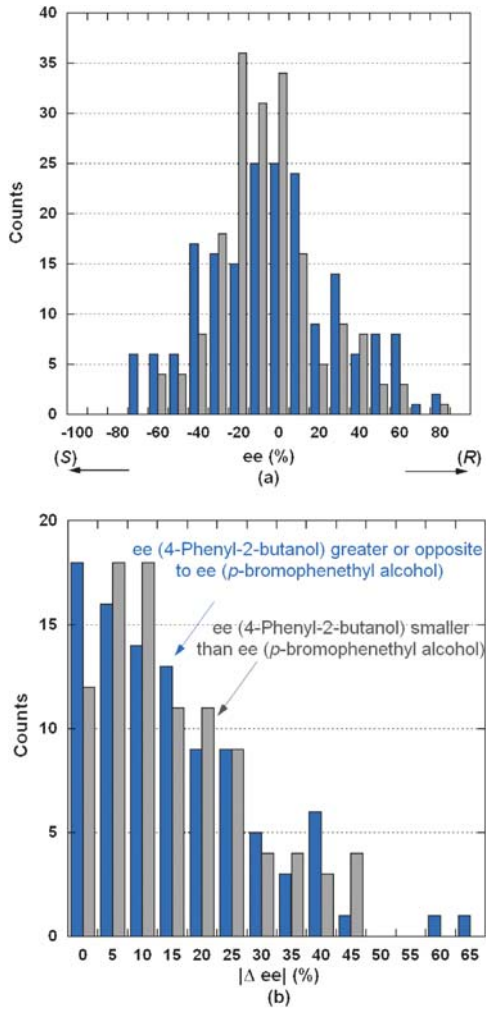

Fig. 6 (a) Enantioselectivity trends for the transfer hydrogenation of substrates **2** and **6** with the immobilized Sav isoforms bearing the 121X (grey bars) and the 124X (blue bars) mutations. (b) Difference in enantiomeric excess (|Δee|) between the aromatic and the aliphatic reduction products, calculated for all the immobilized Sav isoforms.

position 112 may cancel the influence of beneficial K121X or L124X mutations.

(iii) In terms of site of mutation, saturation mutagenesis at position K121 is more effective and creates more diversity than a mutation in position L124 (Fig. 6(a)). It is tempting to speculate that this effect is due to the influence of the K121X side chains both on the piano-stool moiety (K121X from the A monomer) and on the trajectory of the incoming prochiral substrate (K121X from the B monomer, Fig. 4). In the case of the dialkyl substrate, this latter contact may be crucial, as it provides a second coordination sphere interaction with the substrate, reminiscent of the natural enzymes. Using the most efficient protein–ruthenium complexes, the aliphatic ketones **6–8** are reduced with good enantioselectivities (up to 90% ee (*R*) for substrate **7** and 72% ee (*S*) for substrate **6**, Table 4, entries 2–5).

(iv) The designed evolution protocol allows raising the (*S*)-selectivity for the reduction of aromatic substrates from 70% ee (*S*) to 92% ee for substrate **5**.

(v) While a single point mutation is sufficient to generate selective catalysts for the aromatic ketones (>90% ee), double mutants obtained by a designed evolution protocol are required to identify hybrid catalysts for the reduction of dialkyl substrates (up to 90% (*R*)).

(vi) The enantioselectivity obtained for the dialkyl substrates is greater or opposite to the selectivity of aromatic products in more than half of the cases, reaching a |Δee| (difference in enantioselectivity) of up to 65% (Fig. 6(b)). This suggests that protein–substrate interactions, reminiscent of keto-reductases are intimately involved in the enantioselection mechanism as the classical $C_{aromatic}H$–π interaction cannot be implied for dialkyl substrates.

Conclusion

In 1978, Wilson and Whitesides published a visionary, but nearly unnoticed, paper entitled: ''Conversion of a protein to a homogeneous asymmetric hydrogenation catalyst by site specific modification with a diphosphinerhodium(I) moiety''.[25] Inspired by this, we have implemented a chemogenetic scheme for the optimization of artificial metalloenzymes based on the biotin streptavidin technology.

Thus far, this strategy has been successfully applied to the hydrogenation of *N*-protected dehydroaminoacids, the allylic alkylation, alcohol and sulfide oxidation as well as transfer hydrogenation reactions.

In the latter case, and inspired by the X-ray structure of an (*S*)-selective variant, we have implemented an additional designed evolution step that has allowed us to further optimize transfer hydrogenases for the reduction of dialkyl ketones.

Compared to the directed evolution techniques,[66] the designed evolution of artificial metalloenzymes using chemogenetic tools offers new possibilities for protein engineering. Introducing a chemical dimension not only enriches the functionalities of the protein sequence space to be explored, but also represents a variable with a significant impact on the reaction outcome. Variation of the chemical moiety results in a dramatic change in reactivity, as we have demonstrated by implementing very different reactions such as hydrogenation, transfer hydrogenation, oxidation and allylic alkylation using the biotin–streptavidin technology.

The choice of an appropriate host⊂guest couple, the compatibility between the chemical and genetic fragments, as well as the setting up of the reaction conditions are crucial steps for the success of the methodology. Supramolecular anchoring[67–72] appears more promising than either covalent[73–77] or dative[78–84] strategies, since it allows separate variation and characterization, followed by straightforward combination of the chemical and the genetic moieties. A robust protein scaffold and a high affinity between the protein and the organometallic guest are essential parameters. When designed evolution is applied to hybrid metalloenzymes, crystallographic information represents an important input in the system. The general procedure for the designed evolution protocol of an artificial keto-reductase is presented in Scheme 4. The activity and selectivity trends of the reaction are ensured by the choice of the chemical fragment in a first screening round. Since several interactions are involved in the enantioselection mechanism (protein–organometallic fragment and protein–substrate), successive rounds of saturation mutagenesis at

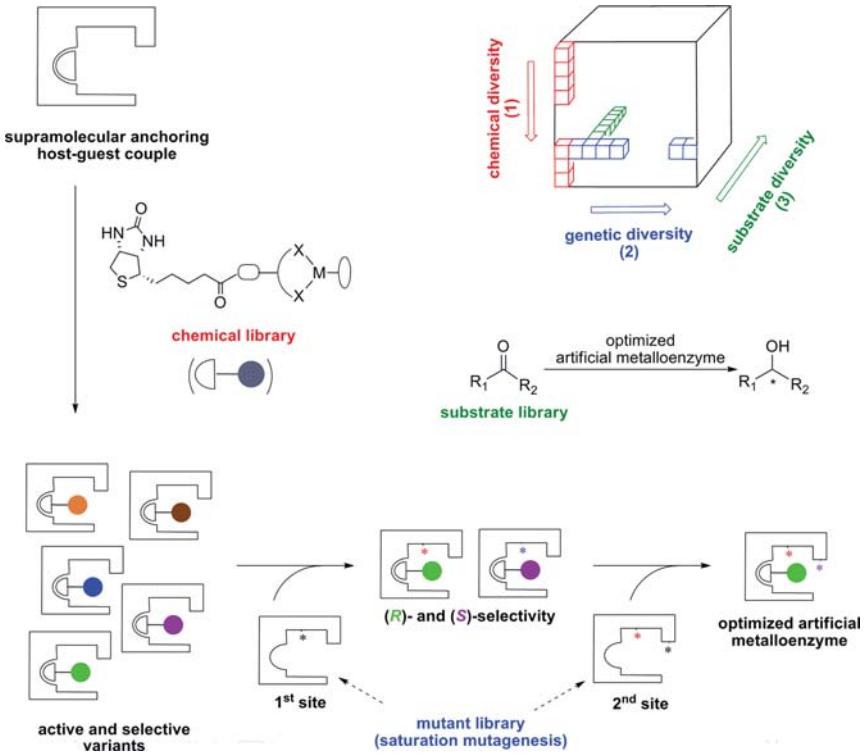

Scheme 4 Designed evolution of an artificial keto-reductase. A search strategy that does not require examination of all possibilities is used to accelerate the chemogenetic optimization procedure.[6] Rational design (choice of mutation sites) and combinatorial methods (structural variation of the chemical component combined with saturation mutagenesis) are used to evolve artificial metalloenzymes with the desired properties.

carefully selected positions of the host protein are necessary to fine-tune the selectivity.

At this stage, the practical use of artificial metalloenzymes is limited due to the high cost of their development and the low activities compared to biocatalysts evolved from natural enzymes. However, their general scope, as well as the rapid optimization procedure makes their application attractive for reactions that are not possible with biocatalysts or for challenging substrates for homogeneous catalysts. The combination of chemical and genetic optimization techniques may result in a quick expansion of protein functionalities and their range of applications. Therefore, we believe that the hybrid catalysts represent a real potential for applications in white biotechnology processes.

All the data accumulated in the past five years demonstrate that such artificial metalloenzymes combine attractive features reminiscent of both homogeneous and enzymatic catalysts. Most notably, the power of exploiting both chemical and genetic optimization allows to rapidly probe the enzyme's fitness landscape.

Current efforts in the group are aimed at extending the concept of artificial metalloenzymes to *in-vivo* catalysis. On one hand, this may allow the use of selection rather than screening to evolve the systems.[85] On the other hand, this may open fascinating perspectives for red biotechnology applications (*i.e.* biomedical applications).

Acknowledgements

This work was funded by the Swiss National Science Foundation (Grants FN 200020-113348), as well as the FP6 Marie Curie Research Training network (MRTN-CT-2003-505020) and the Canton of Neuchâtel. We thank C. R. Cantor for the streptavidin gene.

Notes and references

1 H. U. Blaser, F. Spindler and M. Studer, *Appl. Catal., A*, 2001, **221**, 119–143.
2 A. Thayer, *Chem. Eng. News*, 2006, **84**, 15–25.
3 *Comprehensive Asymmetric Catalysis*, ed. E. N. Jacobsen, A. Pfaltz and H. Yamamoto, Springer, Berlin, 1999.
4 K. Faber, *Biotransformations in Organic Chemistry*, Springer, Berlin, 5th edn, 2004.
5 W. S. Knowles, *Acc. Chem. Res.*, 1983, **16**, 106–112.
6 K. D. Shimizu, M. L. Snapper and A. H. Hoveyda, *Chem.–Eur. J.*, 1998, **4**, 1885–1889.
7 B. Jandeleit, D. J. Schaefer, T. S. Powers, H. W. Turner and W. H. Weinberg, *Angew. Chem., Int. Ed.*, 1999, **38**, 2494–2532.
8 M. T. Reetz, *Angew. Chem., Int. Ed.*, 2001, **40**, 284–310.
9 C. Gennari and U. Piarulli, *Chem. Rev.*, 2003, **103**, 3071–3100.
10 E. M. Vogl, H. Gröger and M. Shibasaki, *Angew. Chem., Int. Ed.*, 1999, **38**, 1570–1577.
11 A. Fersht, *Structure and Mechanism in Protein Science*, W. H. Freeman & Co., New York, 1999.
12 F. H. Arnold and A. A. Volkov, *Curr. Opin. Chem. Biol.*, 1999, **3**, 54–59.
13 O. May, P. T. Nguyen and F. H. Arnold, *Nat. Biotechnol.*, 2000, **18**, 317–320.
14 M. T. Reetz, *Proc. Natl. Acad. Sci. U. S. A.*, 2004, **101**, 5716–5722.
15 R. Berkessel and H. Gröger, *Asymmetric Organocatalysis*, Wiley-VCH, Weinheim, 2004.
16 D. Qi, C. M. Tann, D. Haring and M. D. Distefano, *Chem. Rev.*, 2001, **101**, 3081–3111.
17 Y. Lu, *Curr. Opin. Chem. Biol.*, 2005, **9**, 118–126.
18 C. Letondor and T. R. Ward, *ChemBioChem*, 2006, **7**, 1845–1852.
19 C. M. Thomas and T. R. Ward, *Chem. Soc. Rev.*, 2005, **34**, 337–346.

20 M. Skander, N. Humbert, J. Collot, J. Gradinaru, G. Klein, A. Loosli, J. Sauser, A. Zocchi, F. Gilardoni and T. R. Ward, *J. Am. Chem. Soc*., 2004, **126**, 14411–14418.
21 G. Klein, N. Humbert, J. Gradinaru, A. Ivanova, F. Gilardoni, U. E. Rusbandi and T. R. Ward, *Angew. Chem., Int. Ed*., 2005, **44**, 7764–7767.
22 C. Letondor, A. Pordea, N. Humbert, A. Ivanova, S. Mazurek, M. Novic and T. R. Ward, *J. Am. Chem. Soc*., 2006, **128** 8320–8328.
23 M. Creus and T. R. Ward, *Org. Biomol. Chem*., 2007, **5**, 1835–1844.
24 *Aqueous-Phase Organometallic Catalysis: Concepts & Applications*, ed. B. Cornils and W. A. Herrmann, Wiley-VCH, Weinheim, 2nd edn, 2004.
25 M. E. Wilson and G. M. Whitesides, *J. Am. Chem. Soc*., 1978, **100**, 306–307.
26 *Methods in Enzymology: Avidin-Biotin Technology*, ed. M. Wilchek and E. A. Bayer, Academic Press, San Diego, CA, 1990.
27 A. Loosli, U. E. Rusbandi, J. Gradinaru, K. Bernauer, C. W. Schlaepfer, M. Meyer, S. Mazurek, M. Novic and T. R. Ward, *Inorg. Chem*., 2006, **45**, 660–668.
28 J. Collot, J. Gradinaru, N. Humbert, M. Skander, A. Zocchi and T. R. Ward, *J. Am. Chem. Soc*., 2003, **125**, 9030–9031.
29 C. Letondor, N. Humbert and T. R. Ward, *Proc. Natl. Acad. Sci. U. S. A*., 2005, **102**, 4683–4687.
30 J. Pierron, C. Malan, M. Creus, J. Gradinaru, I. Hafner, A. Ivanova, A. Sardo and T. R. Ward, *Angew. Chem., Int. Ed*., 2008, **47**, 701–705.
31 C. M. Thomas, C. Letondor, N. Humbert and T. R. Ward, *J. Organomet. Chem*., 2005, **690**, 4488–4491.
32 A. Pordea, M. Creus, J. Panek, C. Duboc, D. Mathis, M. Novic and T. R. Ward, *J. Am. Chem. Soc*., 2008, **130**, 8085–8088.
33 M. Yamakawa, I. Yamada and R. Noyori, *Angew. Chem., Int. Ed*., 2001, **40**, 2818–2821.
34 R. Noyori and T. Okhuma, *Angew. Chem., Int. Ed*., 2001, **40**, 40–73.
35 K. Goldberg, K. Schroer, S. Lütz and A. Liese, *Appl. Microbiol. Biotechnol*., 2007, **76**, 237–248.
36 J. C. Moore, D. J. Pollard, B. Kosjek and P. N. Devine, *Acc. Chem. Res*., 2007, **40**, 1412–1419.
37 T. Ohkuma, R. Noyori, H. Nishiyama and S. Itsuno, in *Comprehensive Asymmetric Catalysis*, ed. E. N. Jacobsen, A. Pfaltz and H. Yamamoto, Springer, Berlin, 1999, vol. 1.
38 R. Noyori and S. Hashiguchi, *Acc. Chem. Res*., 1997, **30** 97–102.
39 S. Hashiguchi, A. Fujii, J. Takehara, T. Ikariya and R. Noyori, *J. Am. Chem. Soc*., 1995, **117**, 7562–7563.
40 G. Zassinovich, G. Mestroni and S. Gladiali, *Chem. Rev*., 1992, **92**, 1051–1069.
41 S. Gladiali and E. Alberico, *Chem. Soc. Rev*., 2006, **35**, 226–236.
42 T. Ikariya, K. Murata and R. Noyori, *Org. Biomol. Chem*., 2006, **4**, 393–406.
43 T. Ikariya and A. J. Blacker, *Acc. Chem. Res*., 2007, **40** 1300–1308.
44 M. Yamakawa, H. Ito and R. Noyori, *J. Am. Chem. Soc*., 2000, **122**, 1466–1478.
45 S. E. Clapham, A. Hadzovic and R. H. Morris, *Coord. Chem. Rev*., 2004, **248**, 2201–2237.
46 O. Pàmies and J.-E. Bäckvall, *Chem. Rev*., 2003, **103**, 3247–3262.
47 X. Wu and J. Xiao, *Chem. Commun*., 2007, 2449–2466.
48 X. Wu, X. Li, W. Hems, F. King and J. Xiao, *Org. Biomol. Chem*., 2004, **2**, 1818–1821.
49 X. Wu, X. Li, F. King and J. Xiao, *Angew. Chem., Int. Ed*., 2005, **44**, 3407–3411.
50 S. Ogo, T. Abura and Y. Watanabe, *Organometallics*, 2002, **21**, 2964–2969.
51 K.-J. Haack, S. Hashiguchi, A. Fujii, T. Ikariya and R. Noyori, *Angew. Chem., Int. Ed. Engl*., 1997, **36**, 285–288.
52 K. L. Morley and R. J. Kazlauskas, *Trends Biotechnol*., 2005, **23**, 231–237.
53 M. D. Toscano, K. J. Woycechowsky and D. Hilvert, *Angew. Chem., Int. Ed*., 2007, **46**, 3212–3236.
54 I. Yamada and R. Noyori, *Org. Lett*., 2000, **2**, 3425–3427.
55 R. Noyori, M. Yamakawa and S. Hashiguchi, *J. Org. Chem*., 2001, **66**, 7931–7944.
56 A. Schlatter, M. K. Kundu and W. D. Woggon, *Angew. Chem., Int. Ed*., 2004, **43**, 6731–6734.
57 T. Langer and G. Helmchen, *Tetrahedron Lett*., 1996, **37**, 1381–1384.
58 Y. Arikawa, M. Ueoka, K. Matoba, Y. Nishibayashi, M. Hidai and S. Uemura, *J. Organomet. Chem*., 1999, **572**, 163–168.
59 Y. Nishibayashi, I. Takei, S. Uemura and M. Hidai, *Organometallics*, 1999, **18**, 2291–2293.
60 Y. Jiang, Q. Jiang, G. Zhu and X. Zhang, *Tetrahedron Lett*., 1997, **38**, 215–218.
61 A. M. Hayes, D. J. Morris, G. J. Clarkson and M. Wills, *J. Am. Chem. Soc*., 2005, **127**, 7318–7319.
62 M. T. Reetz and X. Li, *J. Am. Chem. Soc*., 2006, **128** 1044–1045.
63 H. Eklund, B. V. Plapp, J. P. Samama and C. I. Branden, *J. Biol. Chem*., 1982, **257**, 14349–14358.
64 C. A. Voigt, S. L. Mayo, F. H. Arnold and Z. G. Wang, *Proc. Natl. Acad. Sci. U. S. A*., 2001, **98**, 3778–3783.
65 M. Creus, A. Pordea, T. Rossel, A. Sardo, C. Letondor, A. Ivanova, I. Le Trong, R. E. Stenkamp and T. R. Ward, *Angew. Chem., Int. Ed*., 2008, **47**, 1400–1404.
66 M. T. Reetz, J. J.-P. Peyeralans, A. Maichele, Y. Fu and M. Maywald, *Chem. Commun*., 2006, 4318–4320.
67 A. Mahammed and Z. Gross, *J. Am. Chem. Soc*., 2005, **127**, 2883–2887.
68 M. T. Reetz and N. Jiao, *Angew. Chem., Int. Ed*., 2006, **45**, 2416–2419.
69 C.-C. Lin, C.-W. Lin and A. S. C. Chan, *Tetrahedron: Asymmetry*, 1999, **10**, 1887–1893.
70 G. Roelfes and B. L. Feringa, *Angew. Chem., Int. Ed*., 2005, **44**, 3230–3232.
71 G. Roelfes, A. J. Boersma and B. L. Feringa, *Chem. Commun*., 2006, 635–637.
72 D. Coquière, B. L. Feringa and G. Roelfes, *Angew. Chem., Int. Ed*., 2007, **46**, 9308–9311.
73 E. T. Kaiser and D. S. Lawrence, *Science*, 1984, **226** 505–511.
74 R. R. Davies and M. D. Distefano, *J. Am. Chem. Soc*., 1997, **119**, 11643–11652.
75 J. R. Carey, S. K. Ma, T. D. Pfister, D. K. Garner, H. K. Kim, J. A. Abramite, Z. Wang, Z. Guo and Y. Lu, *J. Am. Chem. Soc*., 2004, **126**, 10812–10813.
76 L. Panella, J. Broos, J. Jin, M. W. Fraaije, D. B. Janssen, M. Jeronimus-Stratingh, B. L. Feringa, A. J. Minnaard and J. G. deVries, *Chem. Commun*., 2005, 5656–5658.
77 M. T. Reetz, M. Rentzsch, A. Pletsch and M. Maywald, *Chimia*, 2002, **56**, 721–723.
78 K. Yamamura and E. T. Kaiser, *J. Chem. Soc., Chem. Commun*., 1976, 830–831.
79 T. Kokubo, T. Sugimoto, T. Uchida, S. Tanimoto and M. Okano, *J. Chem. Soc., Chem. Commun*., 1983, 769–770.
80 F. van de Velde, L. Könemann, F. van Rantwijk and R. A. Sheldon, *Chem. Commun*., 1998, 1891–1892.
81 K. Okrasa and R. J. Kazlauskas, *Chem.–Eur. J*., 2006, **12**, 1587–1596.
82 A. Fernández-Gacio, A. Codina, J. Fastrez, O. Riant and P. Soumillion, *ChemBioChem*, 2006, **7**, 1013–1016.
83 T. Ueno, T. Koshiyama, M. Ohashi, K. Kondo, M. Kono, A. Suzuki, T. Yamane and Y. Watanabe, *J. Am. Chem. Soc*., 2005, **127**, 6556–6562.
84 M. Ohashi, T. Koshiyama, T. Ueno, M. Yanase, H. Fujii and Y. Watanabe, *Angew. Chem., Int. Ed*., 2003, **42**, 1005–1008.
85 S. V. Taylor, P. Kast and D. Hilvert, *Angew. Chem., Int. Ed*., 2001, **40**, 3310–3335.